Environmental Earth Sciences (2026) 85:221
https://doi.org/10.1007/s12665-026-12922-4

ORIGINAL ARTICLE

Transboundary hydrogeology and controlling factors of euphrates water chemistry: Insights from hydrochemistry, stable isotopes, and residence times in Syria and Western Iraq

Salih M. Awadh[1] · Mahmood H. D. Al-Kubaisi[2] · Mohd Talha Anees[3] · Ahmad Farid Abu Bakar[3] · Mohammad Ribie Bin Arif[3]

Received: 15 December 2025 / Accepted: 18 March 2026

Abstract

Arid and semi-arid climates are critical for water security in sustainable river systems. The Euphrates River in western Iraq has been increasingly stressed by both geogenic and anthropogenic factors. This study analyzed hydro-geochemical processes, recharge dynamics, and groundwater flow modeling in western Iraq. Additionally, stable isotope tracing ($\delta^{18}O$, Cl^-) integrated with hydro-chemical parameters was used to assess water quality and river-aquifer connectivity in both Syria and western Iraq. A total of 144 groundwater samples were collected annually across 12 stations in western Iraq. Surface water and groundwater data were collected from previous studies at 13 stations in Syria. Results revealed slightly alkaline freshwater conditions (pH 7.6–7.9; TDS 627–888 mg/l), evolution attributed to the dissolution of carbonate and gypsum, agricultural return flows, and industrial effluents. MODFLOW simulations and lumped-parameter modeling indicate bidirectional river–aquifer exchange, with a net river-to-aquifer flux under typical/average hydraulic conditions, although flow may locally reverse toward the river during low-flow periods, with mean residence times of 3–6 years, indicating delayed solute accumulation. Stable isotope enrichment supports evaporative concentration towards the downstream. Overall, the integrated approach reveals spatio-temporal degradation in the Euphrates River water quality controlled by the combined effect of water age, river-aquifer interaction, and anthropogenic inputs. These findings highlighted the need to synchronize monitoring with groundwater age structures and to develop integrated transboundary management strategies for sustainable water use in arid basins.

Keywords Euphrates River · Groundwater flow · Hydrochemistry · Iraq · Stable isotope

Introduction

Surface water and groundwater quantity and quality are generally the key concerns in semi-arid and arid climates, where evaporation is significantly higher than precipitation. In these climates, aquifers are under stress due to over-extraction of groundwater in the agricultural and industrial sectors. The aquifer is also under stress due to complex hydrogeological conditions, including the interaction of surface water and groundwater. This convergence of natural and human-induced stressors poses a significant threat to water security, ecosystem health, and sustainable development, demanding sophisticated methods for assessment and management. The Euphrates River is one of the largest rivers (2718 km long) and most significant waterways in the Middle East and Southwest Asia,

✉ Salih M. Awadh
salih.awadh@sc.uobaghdad.edu.iq

✉ Mohd Talha Anees
talhaanees_alg@yahoo.in

[1] Department of Geology, College of Science, University of Baghdad, Baghdad, Iraq

[2] Department of Applied Geology, College of Science, University of Anbar, Ramadi, Iraq

[3] Department of Geology, Faculty of Science, Universiti Malaya, Kuala Lumpur 50603, Malaysia

Published online: 22 April 2026

flowing southward from its headwaters on the Armenian Plateau through Turkey (28%), Syria (17%), and Iraq (41%) (Hipel et al. 2014; Al-Ansari et al. 2019a). Climatic conditions are semi-arid in the upstream and midstream covering Turkey and parts of Syria, while Iraq has an arid climate. The recharge zone is mainly upstream, where approximately 94% of the discharge originates. That is why evaporation (1300 to 2600 mm yr^{-1} with a mean annual value of 2100 mm) exceeds precipitation (Daggupati et al. 2017). The spatial distribution of precipitation in the upstream (Turkey) and downstream (Iraq) regions shows a declining trend from 931 mm to 97 mm (Tayyeh and Mohammed 2024). River discharge is also in a declining trend from upstream to downstream, which is expected to further decline by approximately 80% in the next two decades (Al-Ansari et al. 2019a). Consequently, the region heavily depends on groundwater for intensive agricultural practices, and a growing industrial sector exemplifies this global challenge.

Previous studies indicate increasing trends in Euphrates River water quality, especially in Iraq. Key physical, chemical, and biological parameters, including pH, electrical conductivity, major ions, biological oxygen demand (BOD), chemical oxygen demand (COD), Fecal Coliform Bacteria (FCB), and E coli, show a relative inclination in concentration from upstream to downstream (Al-Dabbas et al. 2024). Furthermore, the hydraulic connection between the Euphrates River and the underlying aquifer is poorly understood, creating uncertainty in managing surface and groundwater as a single, interconnected resource. Without a holistic understanding of the sources, pathways, and dynamics of these stressors, policymakers and water managers are operating in the dark, implementing mitigation strategies that may be ineffective or even counterproductive.

Groundwater and surface water quality in Iraq is variable and deteriorating due to human activities, geological conditions, and climate change (Ismail et al. 2023). The semi-arid region of Iraq is experiencing a critical water scarcity attributable to several factors, including insufficient water management, the construction of dams on the Tigris and Euphrates rivers in adjacent countries (Iran, Syria, and Turkey), reduced precipitation, and elevated temperatures leading to increased evaporation (Chabuk et al. 2022; Ghalib 2017). As a result, the demand for groundwater for residential, commercial, and agricultural use has increased (Al-Tameemi et al. 2020).

Water quality degradation is assessed by rising salinity and pollution levels, which pose a significant threat to both surface and groundwater resources (Al-Ansari et al. 2019b). As the flow of the Tigris and Euphrates rivers has declined, the salinity of both the water and the land has been progressively increasing. Geological factors, such as salt dissolution or the upward migration of oil field brines, alongside untreated wastewater, solid waste, agricultural runoff (pesticides and fertilizers), and industrial waste (notably from the petroleum sector), frequently contribute to degradation (Al-Tameemi et al. 2020).

Groundwater quality in Iraq exhibits notable variations across different geographic regions and over time. In the northern Kirkuk Governorate, drinking water deteriorated from average (in 2017) to poor (in 2019), including sulfate, TDS, and hardness, due to sewage and oilfield brines (Al-Tameemi et al. 2020; Al-Abadi et al. 2021). Similarly, the water quality of the Shwan and Hawija sub-basins ranges from good to very poor due to anthropogenic sources. However, the sub-basins that recharged from rivers, such as the Lesser Zab River, can have a positive diluting effect (Awadh et al. 2016; Al-Gburi et al. 2023). In central Iraq, Babylon Province classified groundwater as poor to unfit for drinking, primarily due to elevated electrical conductivity and chloride (Chabuk et al. 2022; Al Mousawi et al. 2023). In southern Iraq, the Dammam aquifer in Najaf has poor quality and high TDS. While in the Missan Governorate, 41% of samples are unfit for consumption due to being heavily influenced by the Bazergan oil field (Al-Bahrani et al. 2022; Al-Gburi et al. 2024). The Dibdibba aquifer in Basra is also experiencing water contamination, with water becoming brackish (Al-Mallah et al. 2022). Contrastingly, the Bai-Hassan Formation aquifer in northern Missan and the Western Desert of Al-Anbar provides better water quality, highlighting the role of aquifer lithology and recharge conditions (Al-Gburi et al. 2024; Awadh 2018).

The deterioration of surface water and groundwater quality is getting worse in the main Iraqi river basins. It is worsening due to reduced flow velocities, followed by increasing pollution levels. The Tigris River water quality index indicated good at upstream (e.g., Fishkhabour, Mosul, Tikrit), but gets worse downstream of Baghdad (e.g., Aziziyah, Kut, Amarah) due to rising effluents such as Pb, SO_4^{2-}, and TDS (Al-Ansari et al. 2021). The Euphrates is already salty and undrinkable when it enters Iraq (Al-Ansari et al. 2021). The presence of carcinogenic As and Hg in the Diyala-Sirwan River highlights the severity of wastewater pollution (Issa et al. 2014). In contrast, the Balak Basin in Erbil is typically good, despite turbidity problems (Sh et al. 2024).

The Water Quality Index (WQI) and the Groundwater Quality Index (GWQI) were used to evaluate the suitability of groundwater for drinking or irrigation purposes. Spatial mapping is prevalent in geographic information systems (GIS) in these investigations (Chabuk et al. 2022). These tools have been critical in documenting the widespread degradation, revealing a clear and urgent need for targeted

research and management strategies to address Iraq's multi-faceted water crisis.

Traditional hydrogeological investigations have often relied on isolated methods. Hydro-chemical analysis, including Piper and Gibbs diagrams, has been widely used to identify water types and infer geochemical processes (Davraz and Aksever 2025). Stable isotopes of oxygen ($\delta^{18}O$) and hydrogen ($\delta^{2}H$) have proven invaluable as natural tracers for understanding recharge sources, evaporation processes, and the origin of water (Ren et al. 2024; Karimi et al. 2025). In the realm of quantitative assessment, standard MODFLOW groundwater modeling has been the cornerstone for simulating flow dynamics and predicting aquifer response to pumping (Makhlouf et al. 2024).

Recent studies have begun to integrate these methods. For instance, researchers combine geochemistry with stable isotopes to distinguish anthropogenic nitrate pollution from natural sources. Others have used MODFLOW simulations to quantify the impact of pumping on groundwater levels. However, these integrations are often partial, focusing on either quality or quantity, and frequently lack the explicit incorporation of river-aquifer interaction dynamics, a critical component for holistic basin management.

Despite these advancements, critical gaps remain in complex multi-stressor environments. For example, the integration of hydro-geochemistry and groundwater flow modeling, river-aquifer connectivity, and stress assessment at the regional scale, as well as the contribution of natural and anthropogenic factors to water pollution. Therefore, the purpose of this study is to conduct a comprehensive analysis of the increasing stress on the aquifer system in the Euphrates River catchment. It was executed by developing a novel, integrated methodology that synergistically combines hydro-chemical analysis, groundwater flow modeling, and stable isotope tracing. The specific objectives are (i) to characterize the hydrogeochemical processes and recharge dynamics, (ii) to conduct and analyze a transient groundwater flow model, and (iii) to develop an integrated relationship between hydrochemical, isotopic, and modeling results. This study will provide a robust and transferable framework for integrated groundwater assessment. It will provide water resource managers and policymakers in the Euphrates River catchment with a validated, quantitative tool to test and implement sustainable management scenarios, such as optimized pumping regimes and targeted pollution control measures. Ultimately, this study aims to contribute directly to safeguarding water security and fostering the long-term resilience of the region's aquifer system.

Materials and methods

Study area

The study area spans 455.9 km^2 of the Euphrates River in the Iraqi Western Desert and eastern Syria (Fig. 1).

In Turkey, the Euphrates River originates from two branches, Furat Su and Murad Su, which converge at approximately 3,000 m above mean sea level before flowing 455 km to Jarabulus. It then continues 680 km across Syria and 1,200 km through the Western Desert of Iraq. Near Ramadi, its channel widens and flattens, eventually joining the Tigris at Musayyib to form the Shatt al-Arab (Fig. 1), which discharges into the Arabian Gulf. Seasonal tributaries, such as Al-Maneie and Al-Qaiem, add ephemeral flows to the desert reaches (Al-Kubaisi et al. 2023). Climatic conditions are semiarid (100–150 mm yr^{-1} precipitation; 1600–2200 mm yr^{-1} potential evaporation; mean temperature 19–25 °C). Lithology is primarily Miocene to recent carbonates and gypsum. Throughout its course, the control of water quality is affected by both geogenic and anthropogenic activities. Carbonate dissolution is the main geogenic factor in the Euphrates and Fatha Formations. Whereas, anthropogenic influences include dam operations, agriculture, and industrial discharge (Awadh and Ahmed 2013; Al-Gurairy et al. 2024; Al-Kubaisi 2024). The amount and type of dissolved salts in water determine water quality and influence its intended use (Al-Kubaisi et al. 2022). Despite historical flood events before dam construction, current challenges include reduced flows, salinization, and nutrient loading, all of which threaten the water supply for domestic, agricultural, and hydropower uses (Al-Ansari et al. 2019a; Awadh and Al-Ghani 2014; Awadh et al. 2016). The bedrock underlying the Euphrates River consists primarily of sedimentary strata, with coarse alluvial deposits forming fans where the river exits mountainous terrain in eastern Turkey. Downstream in Syria and Iraq, Miocene carbonates and gypsum of the Euphrates (Lower Miocene) and Fatha (Upper Miocene) Formations predominate (Fig. 2). Terrace formation, meandering patterns, sedimentation, and erosion cycles reflect both natural hydrodynamics and recent land use changes (Awadh and Ahmed 2013).

Limestone dissolution contributes calcium and carbonate ions to the river, increasing hardness and alkalinity, while gypsum and marl from the Fatha Formation release sulfate and increase salinity where groundwater–surface-water exchange occurs. Localized sulfidic springs near Heet further acidify river waters, creating distinct chemistries over short reaches.

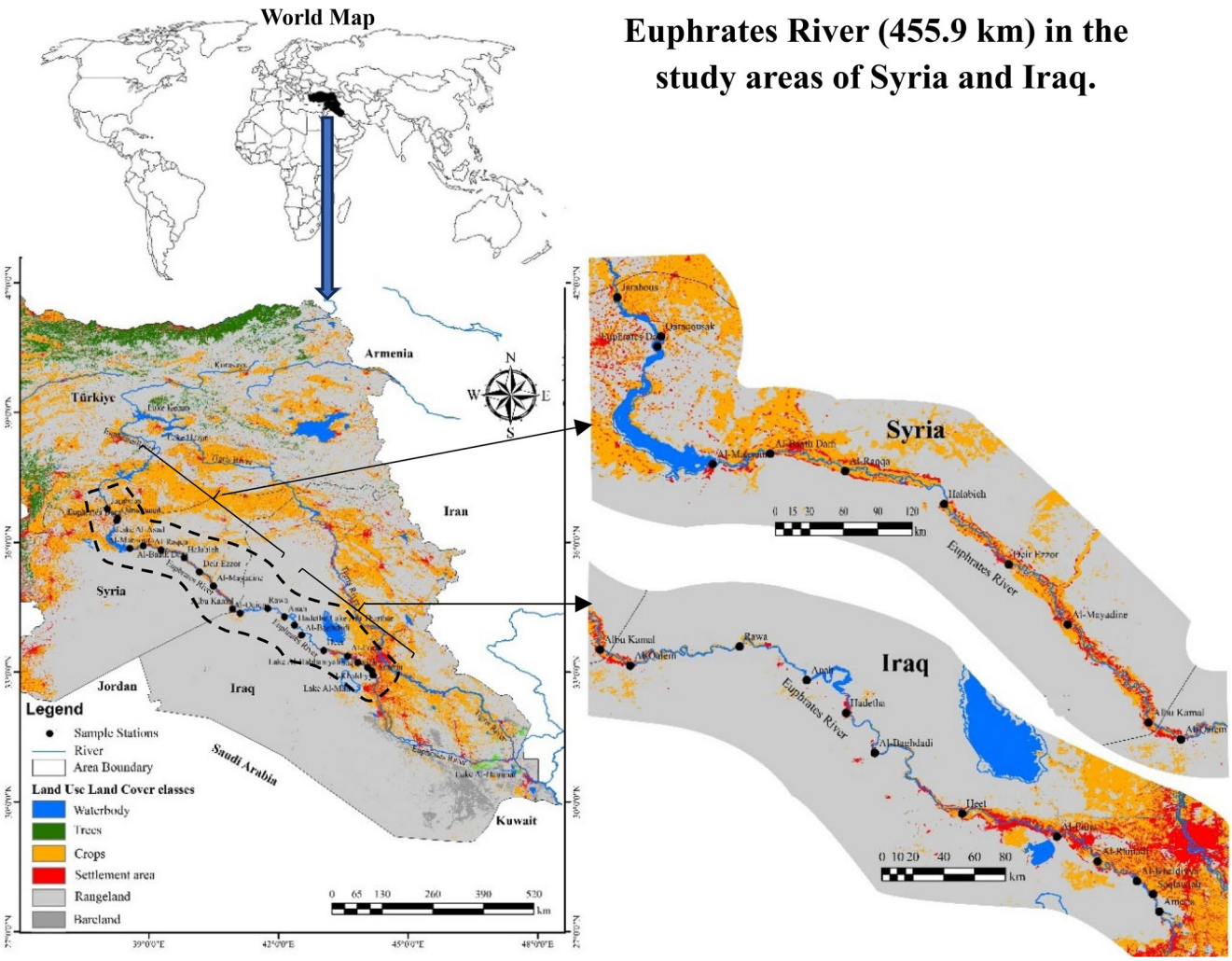

Fig. 1 The base map of the study area and location of water samples along the Euphrates River

Data collection and processing

Rigorous surface-water samples were collected from October 2021 to October 2022 from the Euphrates River system along the Syria-Iraq transboundary zone. Ten (10) monitoring stations in Syria (for stable isotopes) and twelve (12) in Iraq (for hydrochemistry) were identified along the Euphrates River to track changes in surface water chemistry from upstream to downstream. The selection of monitoring stations was based on hydrological features, including river confluences, known discharge stations, dam structures, and ease of collecting water samples. This dataset analysed hydro-chemical changes along the river, sources of contamination, and hydrogeochemical processes that control the water chemistry in the transboundary aquifer. Throughout the year-long trial, 144 surface water samples were collected at a consistent monthly interval. Stable isotope data were collected from a previous study (Kattan 2018). Temporal resolution is crucial for transboundary systems, as upstream alterations, such as dam operations, agricultural water extractions, and water management strategies, can influence the downstream water quality (Ghadimi et al. 2025).

Seasonal fluctuations in physico-chemical properties were considered to accurately comprehend hydrogeochemical processes and determine baseline water chemistry for the Euphrates River system in western Iraq. Physical parameters, such as temperature, electrical conductivity (EC), turbidity, pH, and total dissolved solids (TDS), were measured in the field. The pH was measured using a portable HANNA pH-213 m, which was calibrated daily with standard buffer solutions of pH values 4.01, 7.01, and 10.01. Temperature, TDS, and EC were measured using integrated sensors of the HANNA HI2300 multiparameter probe. Standard coefficients were used to adjust conductivity data for temperature (25 °C) to guarantee consistent results when comparing data from various sampling locations and periods. Turbidity was measured using a HACH 2100 N turbidity

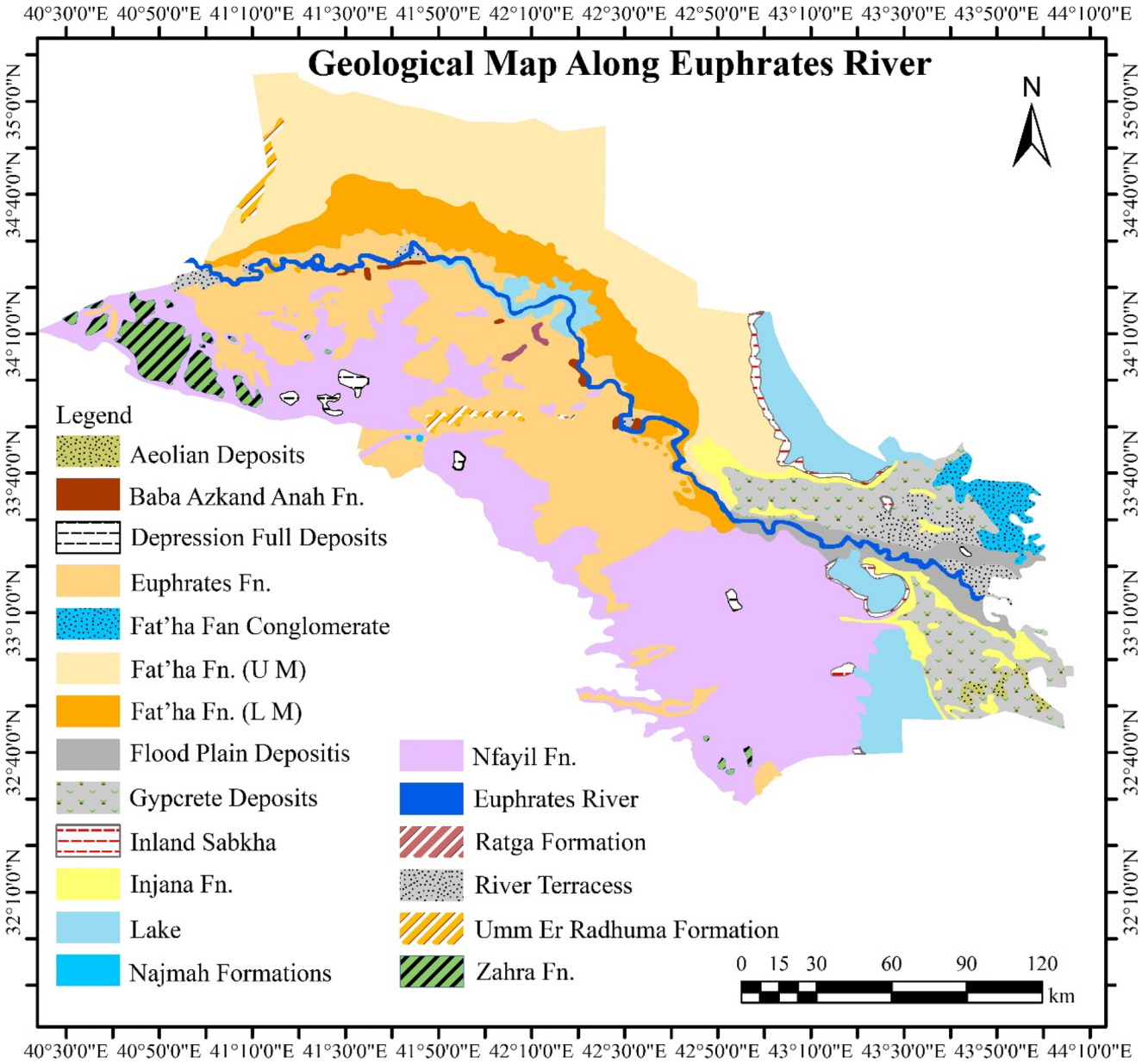

Fig. 2 Geological map of the areas through which the Euphrates River passes in the western desert of Iraq

meter for suspended sediment concentration. Furthermore, instruments were calibrated and cleaned with distilled water before each measurement.

Surface water samples were collected for ion measurement using sterilized 125 mL high-density polyethylene (HDPE) bottles. The samples were filtered using 0.45 µm membrane filters to remove suspended particles and get the dissolved ionic fraction. The filtrates chosen for cation analysis were acidified with a few drops of pure nitric acid (HNO_3) to achieve a pH below 2, thereby preventing metal precipitation and microbial inhibition. All treated samples were stored in cold, dark conditions at 4 °C to prevent physicochemical alterations. The samples were dispatched to the Anbar Water Directorate laboratory within a day (APHA 2017).

The laboratory of the Anbar Water Directorate used internationally accepted and conventional techniques to examine the major ions Ca^{1}, Mg^{2+}, Na^{+}, K^{+}, HCO_3^{-}, CO_3^{2-}, SO_4^{2-}, and Cl^{-}. Every process was performed in compliance with the APHA (1998, 2003) and MGMR (1993) to achieve accurate results and compared with data from other countries. EDTA titration and flame photometry were employed to analyse the principal cations (Ca^{2+}, Mg^{2+}, Na^{+}, K^{+}) using the recognized protocols for water and wastewater analysis (APHA 2017). Anions were measured according to APHA (2017) guidelines and analysed utilizing colorimetric, acid-base,

silver nitrate, and barium chloride titration methods. Total hardness and $CaCO_3$ were evaluated complexometrically with EDTA (Lind 1979). To verify the total ionic concentrations, the TDS were quantified gravimetrically at 105 °C (APHA 2017). The precision of the analysis was assessed by the ionic balance error (IBE) < 5%. (Hounslow et al. 1995). Chloride was measured by silver nitrate titration (APHA 1998); sulfate by $BaCl_2$ precipitation; nitrate and ammonium using Wagtech WTD and Multi Direct kits.

Tracer based resident time analysis

To complement hydro-chemical trends, tracer-based residence time analysis was applied using $\delta^{18}O$ and Cl^-. It allows linking observed downstream solute enrichment with temporal aquifer processes rather than spatial factors. For conservative tracers (Cl^-, $\delta^{18}O$) in a well-mixed system, the mean transit time t approximates:

$$t = Tp + \alpha \tag{1}$$

where *Tp* is the piston delay, and α is the exponential-mixing time constant.

The probability density of groundwater transit times from the river into the aquifer is described by the function:

$$f(t) = 0, \qquad if\ t < Tp \tag{2}$$

For times $t < T_p$, no new river water has yet arrived, so the probability density *f(t)* is zero. For times $t \geq T_p$, water begins to arrive, and the likelihood of arrival at time t follows an exponential decay:

$$f(t) = \frac{1}{\alpha} e^{\left[-\frac{t-T_p}{\alpha}\right]} \tag{3}$$

Groundwater flow modeling and residence time

A two-dimensional, cross-sectional groundwater flow model was developed using MODFLOW v.6.0 to simulate river-aquifer exchange along the western Anbar reach. The model domain represents a vertical section perpendicular to the Euphrates River, extending from the river boundary to the distal aquifer limit and from the ground surface to the base of the unconfined aquifer. The Euphrates River was implemented as a constant-head boundary to represent hydraulic control imposed by river stage. The distal boundary was assigned a no-flow condition to reflect negligible lateral groundwater inflow. The selection of the recharge boundary was based on a distributed flux in regional hydroclimatic conditions. Hydraulic conductivity (Kx, Kz) and storage parameters (Ss) for carbonate–evaporite aquifers were assigned (Li et al. 2023). The estimated riverbed conductance, from sediment characteristics, was used. The simulation of groundwater flow was using the standard flow equation derived from Darcy's law and mass conservation:

$$\frac{\partial}{\partial x}\left(K_x \frac{\partial h}{\partial x}\right) + \frac{\partial}{\partial z}\left(K_z \frac{\partial h}{\partial z}\right) + W = S_s \frac{\partial h}{\partial t} \tag{4}$$

where, h = hydraulic head, K_x, K_y, K_z = hydraulic conductivity in each direction, W = source/sink term (recharge, pumping, river leakage), S_s = specific storage, and t = time. Groundwater velocities are derived from Darcy's law:

$$\vec{v} = -\frac{K}{n} \nabla h \tag{5}$$

where n is the effective porosity. Simulated Darcy velocities averaged 0.2 m/d, corresponding to mean travel distances of approximately 70 m/yr and residence times of 3–5 years across the 300–500 m aquifer thickness. Model calibration performed using observed groundwater heads from monitoring wells along the western Anbar reach. Hydraulic parameters adjusted within physically plausible ranges to minimize discrepancies between simulated and observed heads. Model performance evaluated through head agreement and consistency of simulated river–aquifer exchange with expected field behavior. Simulated travel times were validated independently, comparing them with residence-time estimates, which were calculated from chloride and $\delta^{18}O$ data using an exponential–piston lumped-parameter model (Win BUGS Piston Mix routine). The agreement between numerical and tracer-based results confirmed the model's reliability in representing groundwater flow and river–aquifer interaction. The modeling approach assumes a two-dimensional representation, homogeneous hydraulic properties within layers, and seasonally averaged river stages. The MODFLOW water-budget analysis indicates a positive net exchange from the river to the aquifer under typical hydraulic conditions, confirming the dominance of river leakage toward the groundwater system during the simulation period.

The calibration data, including hydraulic conductivity, storage properties, and riverbed conductance, were obtained from observed groundwater levels from monitoring wells along the western Anbar reach. The data is used to adjust model parameters and evaluate simulated heads. Assessment of model performance was through the agreement between observed and simulated heads to examine the consistency of simulated river–aquifer exchange with expected field behavior. A set of parameters was used for calibration and validation on an independent dataset that included additional groundwater-level measurements and residence-time

estimates derived from chloride and $\delta^{18}O$ lumped-parameter modeling. Close consistency between simulated heads, flow directions, and tracer-based residence times confirmed that the model reliably represents groundwater flow and river-aquifer interaction.

Results and discussion

Spatio-temporal variation of physico-chemical parameters

The relatively high average annual rainfall pattern in Iraq is from October to January. It falls until May, followed by negligible rainfall until September (Al-Ani et al. 2020). The temporal variation of temperature in the study area varies (11 to 34 °C) according to the rainfall pattern, which indicates natural variation. pH levels (6.4 to 8.5) were within the WHO guideline (6.5 to 8.5), but slightly alkaline in the downstream. Electrical conductivity steadily increases from upstream (900 µS/cm) to downstream (1250 µS/cm), reaching the WHO guideline permissible limit (<1500 µS/cm). Total dissolved solids exceeded the acceptable limit (950 mg/l) in the downstream stations (S9 to S12). All stations observed high total hardness, indicating the Euphrates River is hard to very hard. Turbidity values range from 0.4 to 43 NTU, which exceeds the WHO limit (5 NTU) at S2, S6, S10, and S12. These trends were from carbonate dissolution in the Euphrates and Fatha Formations, as well as the input of salts and nutrients through agricultural and industrial effluents (Al-Rawi et al. 2014; Awadh et al. 2013).

Chemical properties (anions and cations) showed a clear increase in pollution gradient downstream. Monitoring stations can be divided into major inflection points, such as S3 and S4, which show initial incidents suggesting first anthropogenic inputs. Station numbers S7 and S8 show significant jumps, indicating major pollution sources, followed by maximum contamination levels from S10 to S12. Sulfate ranged from 215 to 401 mg/l, exceeded 30% to 60% WHO permissible limit (<250 mg/l) consistently towards downstream (Fig. 3). The average concentration of all parameters is given in Table 1.

Major cations (Ca^{2+}, Mg^{2+}, Na^{+}, K^{+}) and anions (Cl^{-}, SO_4^{2-}, HCO_3^{-}) varied longitudinally (Fig. 4). Sulfate (224–366 mg/l; mean 305.6 mg/l) and Ca^{2+} (78–116 mg/l; mean 99.5 mg/l) predominate due to gypsum dissolution in the Fatha Formation. Cl^{-} and Na^{+} co-vary (mean 129.5 mg/l and 106.2 mg/l, respectively), reflecting halite leaching. Salinity in the Euphrates River water depends on the number of dissolved ions, evaporation, and natural and human water inputs. Figures 4 and 5 show the spatial variation of parameters at each station along the Euphrates River. Ternary plots

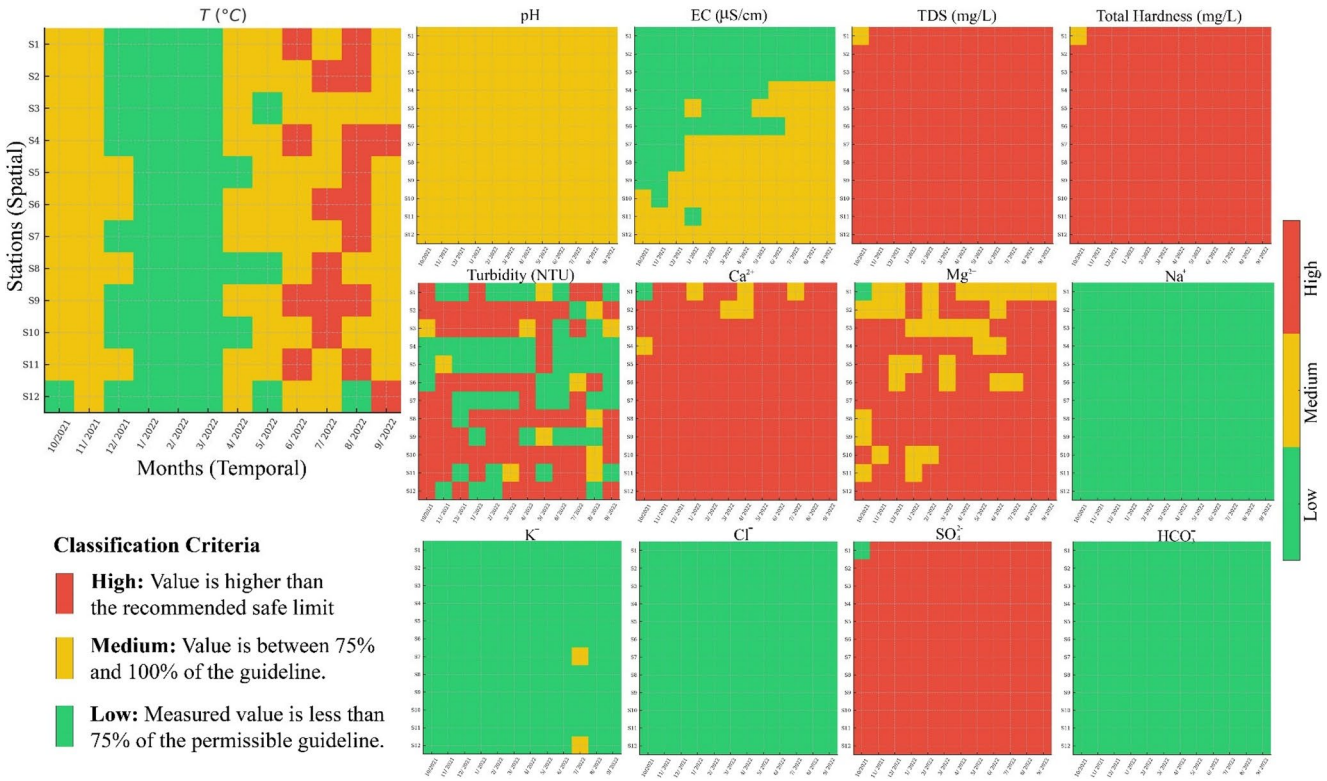

Fig. 3 Heatmap showing monthly (temporal) and station-wise (spatial) variation of 13 physico-chemical parameters. Each plot refers to a parameter. High concentration of ionic parameters indicates groundwater mineralization and anthropogenic inputs

Table 1 Physical and chemical composition of water samples from Euphrates River (October 2021–2022)

Stations	T (°C)	pH	EC (µS/cm)	TDS (mg/l)	TH (mg/l)	Turb. (NTU)	Ca^{2+}	Mg^{2+}	Na^{+}	K^{+}	Cl^{-}	SO_4^{2-}	HCO_3^{-}
Al-Qaiem (S1)	23.42	7.60	895.08	626.56	359.25	3.88	78.25	27.25	82.33	3.79	107.92	224.00	80.83
Rawa (S2)	24.17	7.71	1035.83	725.08	397.75	15.68	81.92	31.83	102.33	5.97	133.00	248.83	97.92
Anah (S3)	22.75	7.61	1067.75	747.43	417.42	7.34	94.83	30.42	106.58	4.49	137.08	259.58	105.83
Haditha (S4)	24.33	7.78	1096.92	767.84	397.08	1.93	91.17	34.00	100.33	5.28	119.25	299.50	107.92
Al-Baghdadi (S5)	24.25	7.95	1116.08	781.26	402.50	2.43	100.58	34.25	99.50	5.28	129.75	293.50	107.67
Heet (S6)	24.67	7.99	1117.75	782.43	416.00	7.92	98.33	31.50	105.00	5.84	129.50	291.00	106.00
Al-Furat (S7)	23.67	7.96	1191.17	833.82	408.83	3.59	98.25	37.33	114.33	5.98	129.50	321.17	108.33
Ramadi (S8)	23.50	7.94	1201.50	841.05	432.58	7.61	103.00	37.08	107.33	5.34	133.50	326.00	107.50
Al-Khalediyya (S9)	23.83	7.91	1222.92	856.04	440.42	6.18	103.42	37.33	112.50	5.68	137.50	334.75	107.25
Saqlawiah (S10)	23.08	7.79	1258.83	881.18	457.50	14.65	115.17	36.83	115.25	5.69	138.00	352.50	104.50
Falluja (S11)	24.92	7.78	1232.67	862.87	465.67	4.81	112.67	35.33	113.00	5.46	128.42	348.92	101.25
America (S12)	20.75	7.75	1268.58	888.01	477.08	8.13	116.08	35.75	116.17	6.28	130.92	366.92	102.50
Min.	20.75	7.60	895.08	626.56	359.25	1.93	78.25	27.25	82.33	3.79	107.92	224.00	80.83
Max.	24.92	7.99	1268.58	888.01	477.08	15.68	116.08	37.33	116.17	6.28	138.00	366.92	108.33
Average	23.61	7.81	1142.09	799.46	422.67	7.01	99.47	34.08	106.22	5.42	129.53	305.56	103.13

(Fig. 6) classify river water as freshwater (TDS < 2000 mg/l), whereas groundwater exhibits brackish to saline signatures (Hem 1985).

Various factors, including geological features, climate, human activities, and interactions with other water bodies, influence the chemistry of the Euphrates River in Iraq. Some hydrocarbon pollutants pollute the Euphrates River in limited areas of Rawa, Hadethah, and Heet (Al-Rawi et al. 2014; Awadh et al. 2013). The water chemistry indicates a high degree of weathering of the bed lithology as the river passes over various geological formations. Overall, the Euphrates River, from upstream to downstream, affects water quality in terms of sulfate and salinity. Other parameters remained below the permissible limit guideline.

River discharge and water shortage

River discharge in the Euphrates is affected by precipitation, floods, droughts, basin topography, and bed permeability. However, upstream dam operations (the GAP project in Turkey), irrigation withdrawals, and industrial use have substantially reduced downstream flow into Syria and Iraq (Yaseen et al. 2018). Long-term drought and altered rainfall patterns under climate change exacerbate water scarcity, decreasing agricultural productivity and threatening food security and public health. In Iraq, the Euphrates inflow is declining from 25.52 km³ to ≈0.24 km³/yr (i.e., 0.96% per year), intensifying competition for limited water resources (Issa et al. 2014).

River-aquifer connectivity

Groundwater flow in western Anbar follows the topographic gradient toward the Euphrates, with recharge occurring during flood pulses and discharge to the river during low stages (Hussein 2010) (Fig. 7). This bidirectional exchange sustains baseflow and supports the local water supply. Under typical hydraulic conditions, the Euphrates predominantly provides net recharge to adjacent aquifers; however, the exchange remains bidirectional, and groundwater discharge toward the river may occur locally during low-flow periods when groundwater heads exceed river stage. However, the net flux is from the river to the aquifer under typical flow conditions. Here, typical flow conditions refer to the representative/average river-stage conditions applied in the baseline MODFLOW simulations (excluding flood-peak pulses and extreme low-stage periods).

Hydrogeological interpretation

Model outputs indicate that the Euphrates River contributes net recharge to the adjacent aquifer under most flow

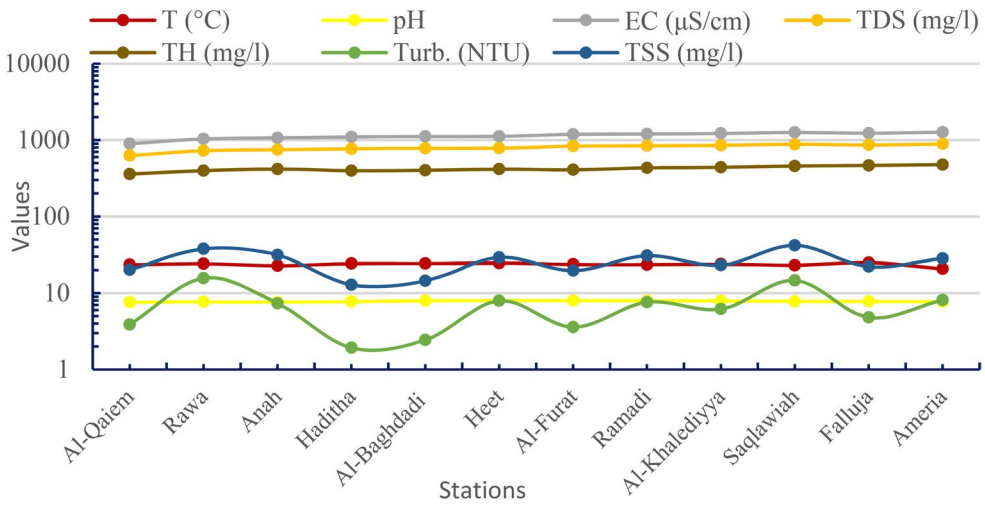

Fig. 4 Spatial distribution of cations and anions showing progressive downstream enrichment related to carbonate and gypsum dissolution

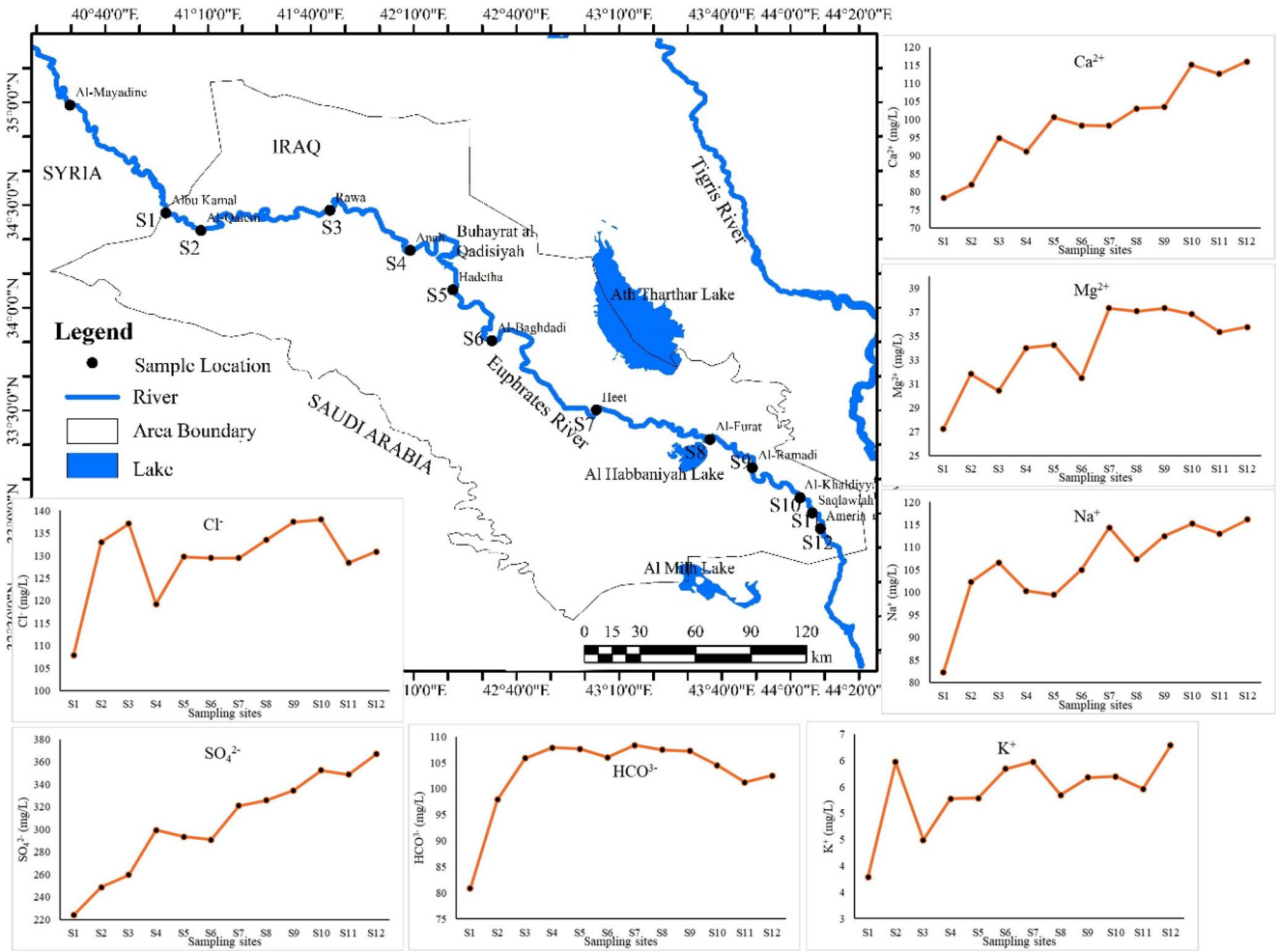

Fig. 5 Spatial distribution of the cations and anions along the Euphrates River

conditions, with peak exchange fluxes of 0.05–0.1 m³/day (Rodell et al. 2004). The calculated travel times (3–5 years) explain the delayed downstream increment in TDS and specific ion ratios relative to seasonal discharge peaks. The pattern supports hydro-chemical and isotopic analyses across the Euphrates Basin (Al-Charideh 2012). The consistency between tracer-derived and model-based residence times underscores the dual influence of carbonate

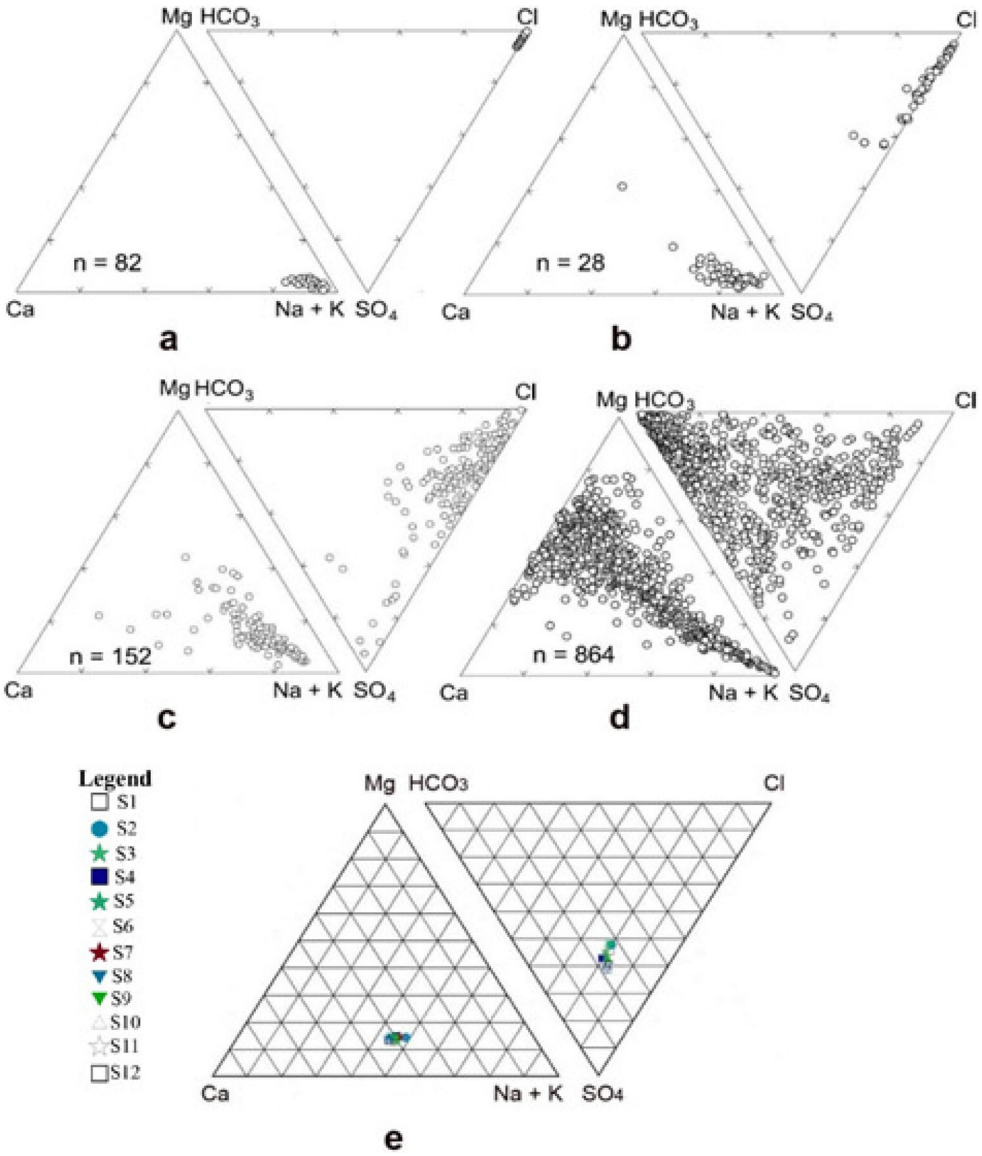

Fig. 6 Ternary plots of cations and anions for waters from the carbonate rock aquifer, using the classification system of Hem (1985); (***a***) brines (>35 000 mg/l), (***b***) saline water (10 000–35 000 mg/l), (***c***) brackish water (2000–10 000 mg/l), (***d***) fresh water (<2000 mg/l), and (**e**) The Euphrates River water (Freshwater). High-TDS waters (a, b, and c) are dominantly Na–Cl, whereas low-TDS waters show a mixing relationship. *n*, number of samples

dissolution and legacy nutrient leaching on water chemistry (Cook and Böhlke 2000; Appelo and Postma 2005). The conceptual cross-section diagram of the river-aquifer model is shown in Fig. 8. In this conceptual model, the Euphrates River stage imposes a hydraulic head that forces water laterally into the underlying unconfined aquifer whenever river levels exceed the local water table, creating a continuous zone of river recharge that gradually diminishes with distance (Winter et al. 1998).

Due to the aquifer's high transmissivity relative to its thickness, advective flow dominates. This flow carries dissolved ions along its paths at an average rate of 0.2 m/day, resulting in multi-year residence times that align with tracer-based estimates (Domenico and Schwartz 1990). Seasonal flood pulses steepen the river–aquifer head gradient, intensifying recharge and accelerating solute transport. Under low-flow conditions, the reduced hydraulic head enables groundwater baseflow to the river, thereby buffering the surface water chemistry against transient variability. These dynamics explain the downstream lag between peaks in discharge and maxima in TDS and specific ion ratios, as water requires several years to traverse the 30 km modelled reach, undergoing progressive geochemical evolution along the way. Similar river–aquifer recharge dynamics with multi-year residence times have been reported in the Indus Basin (Lone et al. 2023), highlighting the importance of time-lagged monitoring in transboundary arid basins.

The estimated residence times (3–6 years) for river-derived recharge in the Euphrates river–aquifer system are consistent with multi-year transit times reported for other arid and semi-arid settings (Lone et al. 2023; Li et al. 2024). However, unlike high-gradient systems, where seasonal recharge signals are transmitted rapidly, the Euphrates reaches exhibit delayed salinity responses driven by

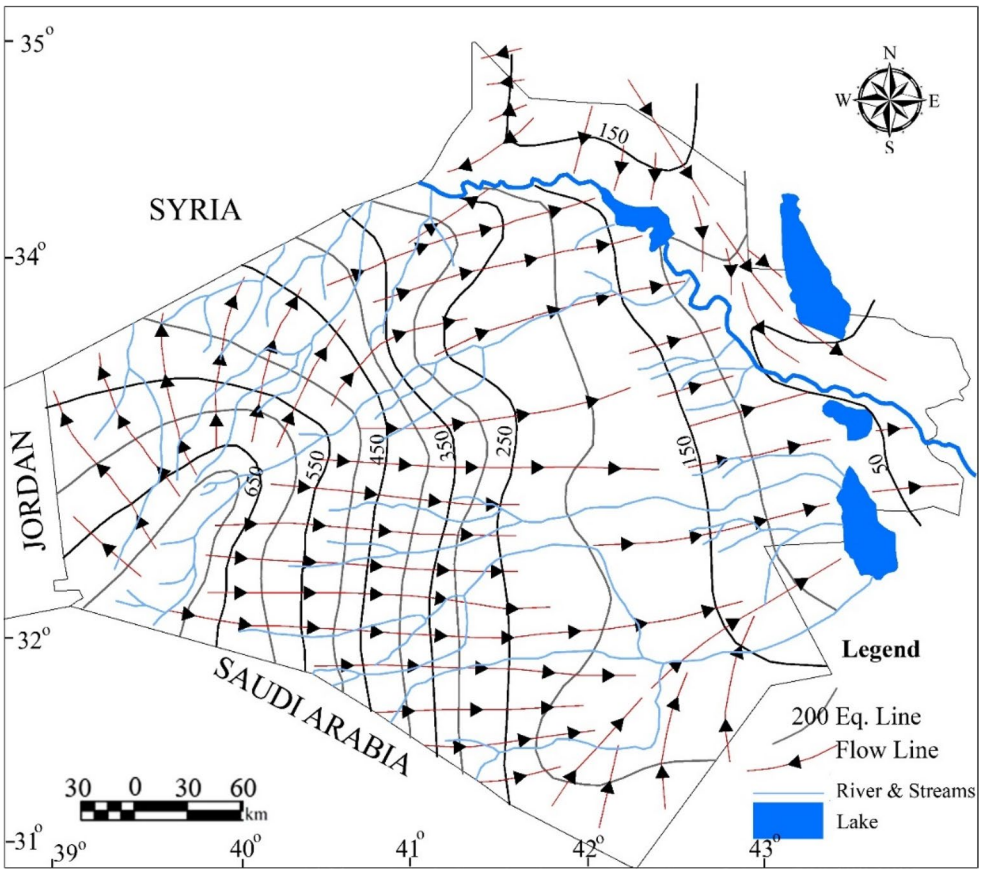

Fig. 7 Conceptual representation of groundwater flow toward the Euphrates River under gaining (low flow) hydraulic conditions, illustrating localized discharge from the aquifer to the river. This scenario differs from the modeled net river-to-aquifer exchange observed under typical hydraulic conditions derived from the MODFLOW water-budget analysis (Hussein 2010)

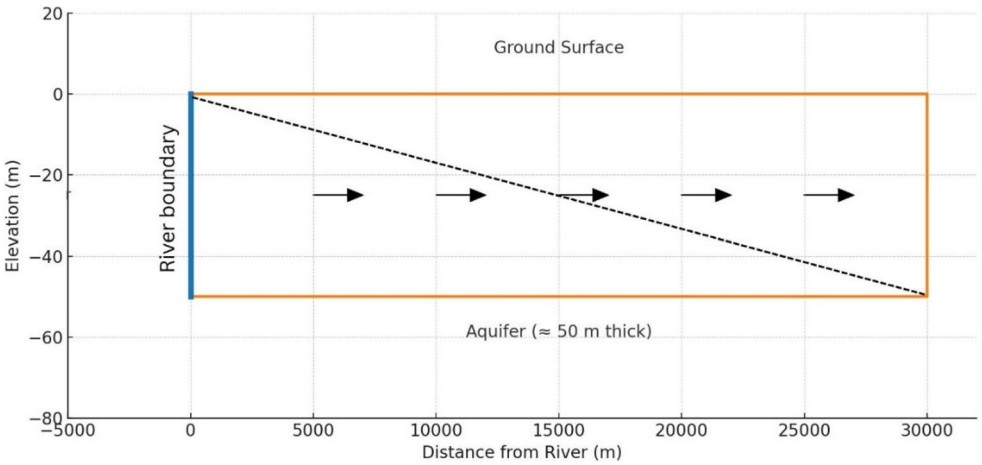

Fig. 8 Conceptual cross-section of the Euphrates River–aquifer system showing boundary conditions, aquifer geometry, and flow directions. River boundary at x = 0 with constant head (blue line), aquifer top and bottom elevations (orange lines), flow direction arrows indicating groundwater movement, aquifer thickness, and ground-surface are labelled

prolonged subsurface storage and evaporative concentration under arid conditions. This behavior is consistent with the river–groundwater interaction framework described by Winter et al. (1998) and implies a relatively strong buffering capacity of the alluvial–carbonate aquifer system. In addition, the progressive downstream increase in sulfate and TDS in Iraq, when viewed alongside the comparatively depleted upstream isotope signatures reported for the Syrian Euphrates sector (Kattan 2018), suggests that hydrochemical evolution is not controlled solely by evaporation. Instead, it reflects the combined effects of cumulative water–rock interaction (Appelo and Postma 2005) and anthropogenic return flows, superimposed on arid-climate concentration processes that are commonly identified using stable isotopes (Ren et al. 2024). These comparisons underscore the value of integrating transient flow modeling with tracer-based age constraints to distinguish spatial contamination sources from time-lagged geochemical responses in transboundary desert basins. Unlike previous studies that addressed hydrochemistry or isotopes separately, this study

quantitatively links transient groundwater flow modeling with tracer-based residence time analysis within a transboundary desert setting.

Conceptual model and transit-time distribution plotted in Fig. 9, based on the exponential–piston lumped-parameter framework. Piston-flow component, where a discrete "slug" of water moves without mixing for a delay time pT, with an exponential-mixing tail, represents gradual dispersive exchange governed by a mixing coefficient α. Here, $pT = 3.63$ years was derived from the Euphrates Formation's bulk density (2.65 g/cm³) and an assumed average Darcy velocity, while $\alpha = 1.5$ years reflects the aquifer's heterogeneity. The resulting probability density function $f(t)$ quantifies the likelihood of water molecules arriving after time t, providing a robust framework for interpreting tracer breakthrough data.

In this study, the model was applied to chloride and $\delta^{18}O$ tracer data to estimate groundwater residence times and validate MODFLOW-derived ages independently. The peaked distribution of residence time at the piston delay and exponentially decayed, indicating most water parcels require 3–6 years to travel from the river into the aquifer and back to sampling points. This temporal framework explains the observed lag between flow variations and progressive increases in dissolved solids and ion ratios downstream. By aligning chemical monitoring intervals with modeled residence times, the research offers actionable guidance for designing sustainable sampling schedules and managing transboundary water quality. A simple exponential–piston lumped-parameter model calibrated to the chloride and $\delta^{18}O$ data from Al-Thawrah, Tabqa, Raqqa, Deir ez-Zor, and Abu-Kamal is shown in Fig. 9.

Tracer age and water interaction

Tracer age results of stable isotopes reveal that groundwater originates in upstream (Syria) either through direct river-aquifer exchange or via irrigation return flow. They also reflect high evaporation effects due to a semi-arid climate and dissolution of salt (Kattan 2015). Total dissolved solids increased from upstream (0.6 mg/l) to downstream (16.5 mg/l), indicating downstream salinization due to irrigation return flow under high evaporation rates. Estimation of groundwater age is modern (<5 to 10 years), based on high tritium (>7 TU) and radiocarbon (>90 pmC) values indicating a recent upstream recharge zone. Kattan (2015) identified chemical evolution in the Euphrates River, showing evolution of water type from Ca-Mg-HCO_3 at upstream to Na-Cl-SO_4 at downstream.

The chloride and $\delta^{18}O$ measurements from Al-Thawrah (107.9 mg/l, −5.12‰), Tabqa (133.0 mg/l, −4.98‰), Raqqa (137.1 mg/l, −4.75‰), Deir ez-Zor (119.3 mg/l, −4.60‰), and Abu-Kamal (129.8 mg/l, −4.45‰) were used to calibrate an exponential–piston lumped-parameter model of the river–aquifer system. In this framework, a discrete piston delay Tp represents the minimum travel time before new Euphrates water influences the aquifer samples. An exponential-mixing term with time constant α describes the dispersive spreading of tracer ages. By matching the downstream enrichment patterns of chloride and the seasonal $\delta^{18}O$ shift, both of which gradually increase with distance from the river, optimal parameter values of $Tp = 3.2$ years and $\alpha = 1.8$ years were determined. The resulting probability density function: The Results of Cl^- and $\delta^{18}O$ of the Euphrates River upstream are mentioned in Table 2.

It predicts that no tracer-bearing water arrives before approximately three years and that transit-time probabilities

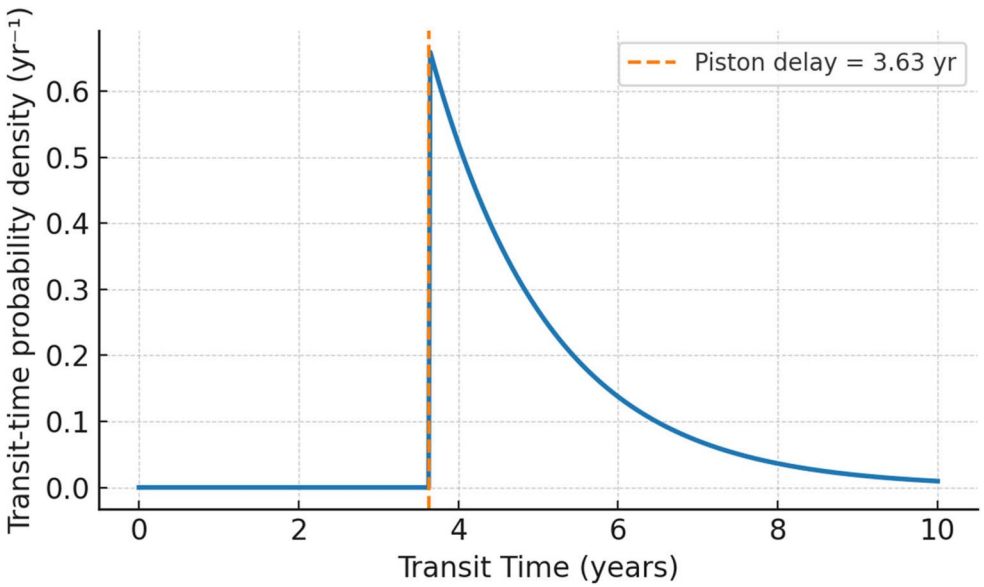

Fig. 9 Transit-time probability distribution for the Euphrates Formation derived from an exponential–piston lumped-parameter model. The vertical dashed line marks the piston-flow delay (3.63 year), after which the probability density follows an exponential decay with mixing time constant (α = 1.5 year)

Table 2 Chloride concentrations and stable-isotope ($\delta^{18}O$) values for the Euphrates River upstream in Syria (after Kattan, 2015)

Location	$\delta^{18}O$ ‰ VSMOW	$\delta 2H$ ‰ VSMOW	Cl- (mg/l)	TDS (mg/l)	EC (µS/cm)
Jarablous	-8.52	-55.1	17.4	242.0	360.0
Qarqosak	-8.39	-54.6	17.9	238.0	353.3
Euphrates Dam	-7.41	-49.1	26.5	272.0	403.0
Al-Mansoura	-7.31	-48.8	29.5	343.0	497.0
Al-Baath Dam	-7.33	-48.5	28.0	273.0	428.0
Al-Raqqa	-7.41	-48.4	36.2	302.0	464.0
Halabieh-Zalabieh	-7.21	-47.9	52.8	407.0	635.0
Deir-Ezzor	-7.24	-48.5	52.9	413.0	641.0
Al-Mayadine	-7.29	-48.1	69.8	476.0	727.0
Albu-Kamal	-7.01	-46.8	86.7	540.0	853.0
Minimum	-8.52	-55.1	17.4	238.0	353.3
Maximum	-7.01	-46.8	86.7	540.0	853.0
Average	-7.51	-49.6	41.8	350.0	536.1

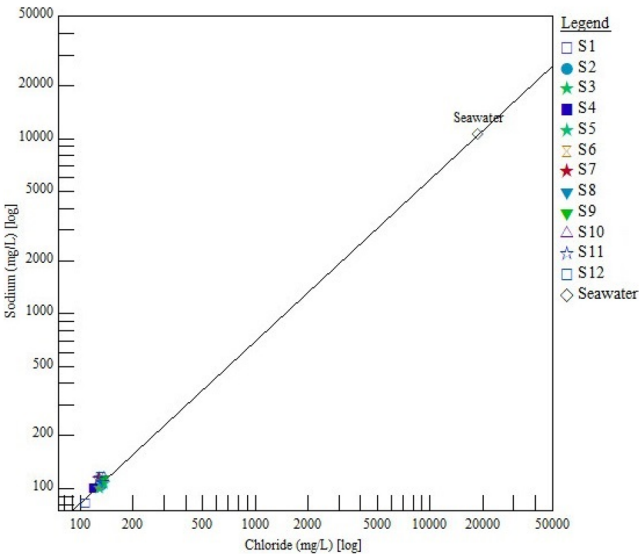

Fig. 10 Plot of Cl versus Na of the Euphrates River water; trend lines are experimentally derived evaporation–dilution curves for seawater (Carpenter 1978)

decay exponentially. This distribution confirms the 2–6 year residence times indicated by the MODFLOW simulation. However, it also provides a quantitative basis for scheduling water-quality sampling at intervals that reflect the actual groundwater-age structure of the Euphrates River and aquifer. In river systems like the Euphrates, analyzing the spatial variation of $\delta^{18}O$ along the river's course can reveal important hydrological processes. The increasing $\delta^{18}O$ values downstream indicate cumulative evaporative enrichment. The Na/Cl ratio of 0.82 mg/l in the Euphrates River is much lower than that of seawater (Fig. 10). Sodium concentrations closely follow chloride, trending along an evaporation-dilution line, indicating water-rock interaction.

Integration of tracer-based results with hydrochemistry of groundwater

The progressive downstream enrichment in Cl^- and $\delta^{18}O$ indicates increasing evaporative influence and cumulative water–rock interaction along the flow path. It aligns with previous studies that show integration of relatively young river water with older groundwater. The chemical evolution of Iraqi groundwater is accelerated and intensified by processes from Syrian groundwater. For instance, TDS increases from 400 mg/l at S1 to 950 mg/l at S12 in Iraq, indicating an exceeding trend from Syria, which may be due to intense evaporation or additional solute inputs. Sulfate downstream dominance also exceeds the permissible limit, likely due to industrial or mining sources. Similarly, gradual shifting of Na^+ to Ca^{2+} from S1 to S12 suggests a longer contact time with aquifer materials. These examples show chemical evolution with the same evaporation, dissolution, and ion exchange processes operating from Syria to Iraq, and further amplified by new pollution inputs. An increase in sulfate sources is also due to industrial or mining activities.

Temporal assessment of simulated groundwater flow in Iraq showing 38% water has less than 3 months transit time, indicating seasonal variations in water quality and rapid contaminant transport. While 15% of water persists for more than a year, and 60% longer transit time in the dry season. It indicates a rapid response to seasonal changes coupled with persistent salinity. Overall, it shows that evaporated irrigation return flow in Syria mixes as baseflow in the downstream of Iraq.

Integrated results suggest three stages of hadrochemical evolution due to mineral dissolution or weathering reactions (Mgbenu and Egbueri 2019). In stage 1 (upstream of Iraq), water type Ca-Mg-HCO_3 originated and was modified through evaporation and irrigation return flow. Evaporation causes a change in the concentration of dissolved ions. However, the sulfate addition was due to anthropogenic activities. These processes transformed the water type to Ca-Mg-HCO_3-SO_4 with sulfate as a dominant anion. Hence, this stage represents the initial anthropogenic impact and low contribution of groundwater dissolution in a naturally controlled system (Sodomon et al. 2025). Stage 2 (midstream of Iraq) indicates sulfate dominance due to the combined effect of evaporation and diffuse agricultural runoff. Stage 3 (midstream to downstream of Iraq) suggests evolution of water type due to industrial and urban wastewater point sources with ion exchange processes in the riverbed and the hyporheic zone. The exchange process of Ca and Mg on clay minerals with Na leads to enrichment of Na in water, resulting in a mixed cation-sulfate water type. These stages clearly show increasing pollution trends downstream

based on the increment in residence time from recharge to discharge areas (Tajbakhshian 2025). It directly correlates with increasing water age, surface and groundwater interaction due to dissolution of evaporite minerals, and increasing anthropogenic activities (Sodomon et al. 2025). The application of fertilizers in agriculture is the main anthropogenic activity that modifies the hydrochemical facies in the region. Long-term monitoring data confirmed the combined effect of mineral dissolution and anthropogenic input in many aquifers of Iraq (Abdullah et al. 2025).

Implications for sustainable groundwater development

This study provides critical insights for the sustainable management of groundwater resources in transboundary arid regions, such as western Iraq, where the Euphrates River plays a dual hydrological role as both a surface watercourse and a hydraulically connected system with adjacent aquifers. MODFLOW-based simulations and residence-time analysis confirm a net-positive river–aquifer exchange. This finding highlighted the need to integrate surface and subsurface water governance frameworks to mitigate the long-term impacts of climate stress and upstream regulation. River–aquifer interaction in the study area is bidirectional and controlled by seasonal variations in the hydraulic gradient between river stage and adjacent groundwater levels, with possible local reversals occurring during low-flow periods.

Groundwater systems in arid environments are particularly sensitive to overexploitation, return flows, and delayed solute migration, which may manifest years after pollutant entry. As emphasized by Gosselin et al. (2017), integrating hydrogeological models with policy instruments is essential for addressing sustainability challenges across regional aquifer systems. Moreover, recent studies by Chen et al. (2020) and Gupta and Sharma (2019) reinforce the importance of groundwater age modeling in shaping sustainable abstraction thresholds, particularly where aquifer vulnerability is exacerbated by rapid salinization or urban encroachment. Findings of this study also align with Li et al. (2024), confirming the use of lumped-parameter models and stable isotope data to refine water-quality monitoring and guide adaptive resource allocation. As groundwater increasingly supplements surface water under variable flow conditions, developing robust transit-time-informed management strategies can protect against cumulative degradation, especially in desert river basins such as the Euphrates corridor.

The identified multi-year groundwater residence times (3–6 years) have direct management implications. Monitoring programs should account for delayed salinity responses, as water-quality changes may reflect recharge conditions from previous years. In active recharge zones, groundwater abstraction should be regulated carefully to prevent accelerated salinization. In irrigation-dominated areas, improved drainage and reduced evaporative losses are essential to mitigate salt accumulation. Given the transboundary nature of the Euphrates Basin, coordinated monitoring and data-sharing mechanisms between Syria and Iraq are critical for sustainable long-term water-quality management.

Conclusions

This study analyzed the hydro-chemical parameters and groundwater flow modeling in western Iraq by integrating stable environmental isotopes in both Syria and Western Iraq. The novelty of this study lies in the integration of stable environmental isotopes in both Syria and western Iraq to identify pollution sources, including isotope residence times and seasonal transit delays. The hydro-chemical characterization of the Euphrates River within the western Iraqi desert reveals that both natural and anthropogenic mechanisms significantly shape the observed water quality patterns. Key geogenic controls include the dissolution of carbonate and evaporite formations, particularly from the Euphrates and Fatha units, which contribute substantial calcium, bicarbonate, and sulfate to the river load. Simultaneously, agricultural and industrial discharges increase nutrient and salinity levels downstream. MODFLOW and lumped-parameter modeling indicate that the river–aquifer system exhibits bidirectional hydraulic exchange, with a net river-to-aquifer flux occurring under typical hydraulic conditions. Localized or seasonal reversals toward the river may occur during the low-flow periods. The estimated residence times of 3–5 years regulate the delayed response in solute concentrations. Stable isotope signatures ($\delta^{18}O$) and conservative tracer behavior (Cl^-) support these findings by explaining the dynamics behind the chemical evolution of the water. The seasonal response of the stable isotope indicated an increasing mean water transit time (2 to 8 months) in the downstream. Overall, the main water stress is due to both geogenic and anthropogenic factors. This research highlighted the necessity of synchronizing sampling regimes with modeled groundwater age distributions to improve monitoring accuracy. Collectively, the results advocate for integrated water resource strategies that account for both surface and subsurface hydrological interactions across transboundary desert basins. However, this study is limited by uneven isotope data across the transboundary, avoids complex flows during simulations, and has a limited focus on specific contaminants from point sources. Furthermore, this study recommends synchronized monitoring with an increment of temporal data, Syrian-Iraqi strategies for

upstream activities, joint water sharing and quality agreements, and simultaneously focus on both natural and anthropogenic sources.

Acknowledgements The authors gratefully acknowledge the local communities for their logistical support and the staff of the Anbar Water Directorate for their assistance with sample analysis. We also acknowledge the Department of Applied Geology, College of Science, University of Anbar, for collaboration with the Department of Geology, Faculty of Science, Universiti Malaya. The authors would also like to acknowledge the support provided by the ongoing Universiti Malaya Research Excellence Grant (UMREG023-2024) provided by the Research Grant Management Division, Universiti Malaya.

Authors' contributions S.M.A. conceived the study, processed and interpreted the data, and drafted the manuscript. M.H.D.A. performed field sampling, prepared figures, and maps. M.T.A re-drafted the manuscript and prepared it according to journal guidelines. M.R.B.A wrote a part about methodology and results. A.F.B.A.B supervised the work. All authors reviewed and approved the final manuscript.

Funding This research received no specific grant from any funding agency in the public, commercial, or not-for-profit sectors.

Data availability No datasets were generated or analysed during the current study.

Declarations

Competing interests The authors declare no competing interests.

References

Abdullah MA, Jemaa NC, Saleh SA (2025) Controls on groundwater quality: Hydro-Morphometric, Stratigraphic, Structural & Isotopic indicators, Al-Jirnaf Valley watershed, Iraq. Carbonates Evaporites 40(3):112. https://doi.org/10.1007/s13146-025-01144-7

Al-Abadi AM, Fryar AE, Rasheed AA, Pradhan B (2021) Assessment of groundwater potential in terms of the availability and quality of the resource: a case study from Iraq. Environ Earth Sci 80(12):426. https://doi.org/10.1007/s12665-021-09725-0

Al-Ani IA, Al-Thamery HA, Al-Ansari N, Al-Janabi AM, Mohtar WH (2020) Multi criteria decision making to optimize the best runoff control measures for the Haditha Dam Reservoir, Iraq. J Environ Hydrology 28(4):1–14. https://www.diva-portal.org/smash/get/diva2:1477234/FULLTEXT01.pdf Accessed 16 Dec 2025

Al-Ansari N, Adamo N, Sissakian V (2019a) Hydrological characteristics of the Tigris and Euphrates Rivers. J earth Sci Geotech Eng 9(4):1–26. https://www.diva-portal.org/smash/get/diva2:1369432/FULLTEXT01.pdf Accessed 16 Dec 2025

Al-Ansari N, Jawad S, Adamo N, Sissakian V (2019b) Water quality and its environmental implications within Tigris and Euphrates rivers. J earth Sci Geotech Eng 9(4):57–108. https://www.diva-portal.org/smash/get/diva2:1369452/FULLTEXT01.pdf Accessed 16 Dec 2025

Al-Ansari N, Saleh S, Abdullah T, Abed SA (2021) Quality of surface water and groundwater in Iraq. Earth Sci Geotech Eng 11(2):161–199. https://doi.org/10.47260/jesge/1124

Al-Bahrani HS, Al-Rammahi AH, Al-Mamoori SK, Al-Maliki LA, Al-Ansari N (2022) Groundwater detection and classification using remote sensing and GIS in Najaf, Iraq. Groundw Sustainable Dev 19:100838. https://doi.org/10.1016/j.gsd.2022.100838

Al-Charideh A (2012) Geochemical and isotopic characterization of groundwater from shallow and deep limestone aquifers system of Aleppo basin (north Syria). Environ Earth Sci 65(4):1157–1168. https://doi.org/10.1007/s12665-011-1364-6

Al-Dabbas MA, Al-Ali IA, Husain MM (2024) Water quality assessment of the euphrates river from haditha to Al-Nasiriyah, Iraq. Iraqi Geol J. https://doi.org/10.46717/igj.57.2B.18ms-2024-8-28. 31:272–85

Al-Gburi HF, Al-Ali IA, Dar FA, Al-Sheikh ON (2024) Groundwater quality assessment and pollution sources identification using statistical analyses at Missan Governorate, Southeast Iraq. Discover Sustain 5(1):416. https://doi.org/10.1007/s43621-024-00578-8

Al-Gburi HF, Al-Tawash BS, Al-Tamimi OS, Schüth C (2023) Impacts of hydrogeochemical processes and land use practices on groundwater quality of Shwan sub-Basin. Kirkuk North Iraq Heliyon 9:e13995. https://doi.org/10.1016/j.heliyon.2023.e13995

Al-Gurairy A, Al-Jubory MS, Al-Ansari N, Muhammad Awadh S, Al-Zubaidi AH, Al-Sadun MT, Al-Ghurairy RM (2024) Tectonic activation and the risk of Ilisu Dam collapse to Iraq through modelling and simulation using HEC-RAS. Appl water Sci 14(11):240. https://doi.org/10.1007/s13201-024-02299-9

Al-Kubaisi MH (2024) Surface runoff estimation in kubaisa watershed using SWAT, Western Desert, Iraq. The Iraqi Geological Journal 31:286–97. https://doi.org/10.46717/igj.57.2B.19ms-2024-8-29

Al-Kubaisi MH, Al-Salmani NZ, Mohammad OJ, Fayyadh AM, Orabi OH (2022) Evaluation of irrigation water quality index (IWQI) for Habbaniya lake in Anbar Governorate, Iraq. In IOP Conference Series: Earth and Environmental Science 1080(1):012019. IOP Publishing. https://doi.org/10.1088/1755-1315/1080/1/012019

Al-Kubaisi MH, Fayyadh AM, Al-Sumaidai SK, Ameen BK (2023) Validity of Euphrates River Water within Anbar Governorate, Iraq. Iraqi Geol J 25:64–79. https://doi.org/10.46717/igj.56.1F.5ms-2023-6-13

Al-Mallah IA, Al-Qurnawi WS, Ghalib HB, Al Hawash AB, Abdulameer MH (2022) Evaluation of groundwater quality in the Dibdibba aquifer using hydrogeochemical and isotope techniques (Basrah Province, Iraq). Acta Geochim 41(5):823–838. https://doi.org/10.1007/s11631-022-00549-8

Al Mousawi E, Jahad UA, Mahmoud AS, Chabuk A, Naje AS, Al-Ansari N, Laue J (2023) Implementation of the quality and creating GIS maps for groundwater in Babylon, Iraq. J Ecol Eng 24(8):310–321. https://doi.org/10.12911/22998993/166392

Al-Rawi FR, Al-Ameri TK, Awadh SM (2014) Petroleum geochemistry of oil samples from shallow boreholes at Sakran site, western Iraq. Arab J Geosci 7(2):545–558. https://doi.org/10.1007/s12517-012-0813-1

Al-Tameemi IM, Hasan MB, Al-Mussawy HA, Al-Madhhachi AT (2020) Groundwater Quality Assessment Using Water Quality Index Technique: A Case Study of Kirkuk Governorate, Iraq. In IOP Conference Series: Materials Science and Engineering 881(1):012185. IOP Publishing. https://doi.org/10.1088/1757-899X/881/1/012185

APHA (1998) Standard Methods for the Examination of Water and Wastewater, 20th edn. American Public Health Association, Washington, DC

APHA (2003) Standard Methods for the Examination of Water and Wastewater, 21st edn. American Public Health Association, Washington, DC

APHA (2017) Standard Methods for the Examination of Water and Wastewater, 23rd edn. American Public Health Association, Washington DC

Appelo CAJ, Postma D (2005) Geochemistry, groundwater and pollution, 2nd edn. CRC Press/Balkema, Leiden. Chapter 7

Awadh SM (2018) A preliminary assessment of the geochemical factors affecting groundwater and surface water quality around the rural communities in Al-Anbar, Western Desert of Iraq. Environ Earth Sci 77(3):83. https://doi.org/10.1007/s12665-018-7262-4

Awadh SM, Ahmed RM (2013) Hydrochemistry and pollution probability of selected sites along the Euphrates River, western Iraq. Arab J Geosci 6:2501–2518. https://doi.org/10.1007/s12517-012-0538-1

Awadh SM, Al-Ghani SA (2014) Assessment of sulfurous springs in the west of Iraq for balneotherapy, drinking, irrigation and aquaculture purposes. Environ Geochem Health 36:359–373. https://doi.org/10.1007/s10653-013-9555-6

Awadh SM, Ali KK, Alazzawi AT (2013) Geochemical exploration using surveys of spring water, hydrocarbon and gas seepage, and geobotany for determining the surface extension of Abu-Jir Fault Zone in Iraq: A new way for determining geometrical shapes of computational simulation models. J Geochem Explor 124:218–229. https://doi.org/10.1016/j.gexplo.2012.10.011

Awadh SM, Al-Kilabi JA, Abdulhussein FM (2016) Assessment of groundwater quality using water quality indexin, Al-Hawija area, northern Iraq. Iraqi Geol J 2016:67–76. https://doi.org/10.46717/igj.39-49.1.5Ms-2016-06-27

Carpenter AB (1978) Origin and chemical evolution of sedimentary brines in sedimentary basins. Okla Geol Surv Circular 79:60–77. https://doi.org/10.2118/7504-MS

Chabuk A, Jahad UA, Majdi A, Isam M, Al-Ansari N, Majdi SH, Laue H, Abed J SA (2022) Creating the Distribution Map of Groundwater for Drinking Uses Using Physio-Chemical Variables; Case Study: Al-Hilla City. Iraq Water Air Soil Pollution 233(6):218. https://doi.org/10.1007/s11270-022-05660-3

Chen X, Jiang J, Lei T, Yue C (2020) GRACE satellite monitoring and driving factors analysis of groundwater storage under high-intensity coal mining conditions: A case study of Ordos, northern Shaanxi and Shanxi, China. Hydrogeol J 28(2):673–686. https://doi.org/10.1007/s10040-019-02101-0

Cook PG, Böhlke JK (2000) Determining timescales for groundwater flow and solute transport. Environmental tracers in subsurface hydrology 1–30. Springer US, Boston, MA

Daggupati P, Srinivasan R, Ahmadi M, Verma D (2017) Spatial and temporal patterns of precipitation and stream flow variations in Tigris-Euphrates river basin. Environ Monit Assess 189(2):50. https://doi.org/10.1007/s10661-016-5752-y

Davraz A, Aksever F (2025) Geochemical processes in groundwater chemistry: a case study. Carbonates Evaporites 40(3):92. https://doi.org/10.1007/s13146-025-01124-x

Domenico PA, Schwartz FW (1990) Physical and Chemical Hydrogeology. Wiley, New York

Ghadimi S, Sharifi A, Ahrari A, Mazaheri M, Noury M, Klöve B, Torabi Haghighi A (2025) From upstream development to downstream water shortage: tracing hydrological changes in the Karkheh River Basin. Sustainable Water Resour Manage 11(5):87. https://doi.org/10.1007/s40899-025-01266-9

Ghalib HB (2017) Groundwater chemistry evaluation for drinking and irrigation utilities in east Wasit province, Central Iraq. Appl Water Sci 7(7):3447–3467. https://doi.org/10.1007/s13201-017-0575-8

Gosselin DC, Sibray SS, Ayers JF (2017) A Review of Hydrogeologic Characteristics of the High Plains Aquifer, USA. In A. J. Welch & K. G. Mumma (Eds.), Proceedings of the 10th International Symposium on Managed Aquifer Recharge (ISMAR10), National Groundwater Association 196–205

Gupta PK, Sharma D (2019) Assessment of hydrological and hydrochemical vulnerability of groundwater in semi-arid region of Rajasthan, India. Sustainable Water Resour Manage 5(2):847–861. https://doi.org/10.1007/s40899-018-0260-6

Hem JD (1985) Study and Interpretation of the Chemical Characteristics of Natural Water. US Geological Survey Water-Supply Paper 2254

Hipel KW, Kilgour DM, Kinsara RA (2014) Strategic investigations of water conflicts in the Middle East. Group Decis Negot 23(3):355–376. https://doi.org/10.1007/s10726-013-9362-0

Hounslow A 1995. Water Quality Data: Analysis and Interpretation. Lewis, Boca Raton, FL

Hussien BM (2010) Hydrogeologic condition within al-Anbar governorate. J Anbar Univ pure Sci 4(3):97–111. https://www.researchgate.net/profile/Bayan-Hussien/publication/303909919_HYDROGEOLOGIC_CONDITIONS_WITHIN_AL-ANBAR_GOVERNORATE/links/575c2afd08aec91374abc09d/HYDROGEOLOGIC-CONDITIONS-WITHIN-AL-ANBAR-GOVERNORATE.pdf Accessed 16 Dec 2025

Ismail AH, Shareef MA, Hassan G, Alatar FM (2023) Hydrochemistry and water quality of shallow groundwater in the Tikrit area of Salah Al Din Province, Iraq. Appl Water Sci 13(10):197. https://doi.org/10.1007/s13201-023-02008-y

Issa IE, Al-Ansari N, Sherwany G, Knutsson S (2014) Expected future of water resources within Tigris–Euphrates rivers basin, Iraq. J Water Resour Prot 6(5):421–432. https://doi.org/10.1007/s13201-021-01397-2

Karimi O, Noori R, Javadi S, Jun C, Bateni SM, Choubin B, Noury M, Heydarizad M, Kianmehr P, Tang Q, Huneau F (2025) A dataset of water stable isotopes in Iran's main aquifers. Sci Data 12(1):1724. https://doi.org/10.1038/s41597-025-06000-w

Kattan Z (2015) Chemical and isotopic characteristics of the Euphrates River water, Syria: Factors controlling its geochemistry. Environ Earth Sci 73(8):4763–4778. https://doi.org/10.1007/s12665-014-3762-z

Kattan Z (2018) Using hydrochemistry and environmental isotopes in the assessment of groundwater quality in the Euphrates alluvial aquifer. Syria Environ earth Sci 77(2):45. https://doi.org/10.1007/s12665-017-7197-1

Li M, Xie Y, Dong Y, Wang L, Zhang Z (2024) Recent progress on groundwater recharge research in arid and semiarid areas of China. Hydrogeol J 32(1):9–30. https://doi.org/10.1007/s10040-023-02656-z

Lind OT (1979) Handbook of Common Methods in Limnology. *C.V.* Mosby Company, Burlington, VT

Li Y, Shu L, Wu P, Zou Z, Lu C, Liu B, Niu S, Yin X (2023) Influence of the karst matrix hydraulic conductivity and specific yield on the estimation accuracy of karstic water storage variation. J Hydrol 626:130186. https://doi.org/10.1016/j.jhydrol.2023.130186

Lone SA, Jeelani G, Deshpande RD, Bhat MS, Padhya V (2023) Assessing the hydrological controls on spatio-temporal patterns of stream water in glacierized mountainous Upper Indus River Basin (UIRB), western Himalayas. J Hydrol 619:129310. https://doi.org/10.1016/j.jhydrol.2023.129310

Makhlouf A, El-Rawy M, Kanae S, Ibrahim MG, Sharaan M (2024) Integrating MODFLOW and machine learning for detecting optimum groundwater abstraction considering sustainable drawdown and climate changes. J Hydrol 637:131428. https://doi.org/10.1016/j.jhydrol.2024.131428

Mgbenu CN, Egbueri JC (2019) The hydrogeochemical signatures, quality indices and health risk assessment of water resources in Umunya district, southeast Nigeria. Appl Water Sci 9:1–19. https://doi.org/10.1007/s13201-019-0900-5

Ministry of Geology and Mineral Resources of the People's Republic of China (1993) Testing Methods of Underground Water Quality—Determination of Carbonate, Bicarbonate and Hydroxide-Titrimetric (DZ/T0064.49-93). China Standards, Beijing, China

Ren X, Li P, He X, Zhang Q (2024) Tracing the sources and evaporation fate of surface water and groundwater using stable isotopes of hydrogen and oxygen. Sci Total Environ 931:172708. https://doi.org/10.1016/j.scitotenv.2024.172708

Rodell M, Famiglietti JS, Chen J, Seneviratne SI, Viterbo P, Holl S, Wilson CR (2004) Basin scale estimates of evapotranspiration using GRACE and other observations. Geophysical Research Letters. 31(20): L20504(1–4). https://doi.org/10.1029/2004GL020873

Sh AJ, Dara RN, Chnaray MA, Ahmed AR, Khoshnaw HS (2024) HYDROCHEMICAL STUDY OF BALAK RIVER, ERBIL-IRAQ. Iraqi J Agricultural Sci 55(5):1743–1755. https://doi.org/10.36103/mrsdd983

Sodomon AK, Akpataku KV, Tampo L, Mande SL, Herrera JB, Rosales WM, Faye S (2025) Assessment of hydrogeochemical evolution of groundwater from the basement aquifer in the upper part of transboundary Mono River Basin, Togo. J Hydrology: Reg Stud 58:102200. https://doi.org/10.1016/j.ejrh.2025.102200

Tajbakhshian M (2025) Integrated hydrogeochemical and spatial assessment of groundwater quality using multivariate statistics and GIS: a case study from northeastern Iran. Environ Syst Res 14(1):19–11. https://doi.org/10.1186/s40068-025-00412-8

Tayyeh HK, Mohammed R (2024) Trend analysis of hydrometeorological data in Euphrates river Basin. Environ Earth Sci 83(24):676. https://doi.org/10.1007/s12665-024-12002-5

Winter TC, Harvey JW, Franke OL, Alley WM (1998) Groundwater and surface water: A single resource. US Geol Surv Circular 1139

Yaseen ZM, Awadh SM, Sharafati A, Shahid S (2018) Complementary data-intelligence model for river flow simulation. J Hydrol 567:180–190. https://doi.org/10.1016/j.jhydrol.2018.10.020